Mapana – Journal of Sciences
2026, Vol. 25, No. 1, *1-17*
ISSN 0975-3303 | https://doi.org/10.12723/mjs.76.1

Physical, Structural, Thermal, electrical and dielectric investigations on Li_2O doped Borosilicate Glasses

Aravind Dyama*, T. Sankarappa*, Pallavi Jamadar*, Mohansingh Heerasingh*, R. Ramanna†

Abstract

Li_2O-doped borosilicate glasses were prepared. They were confirmed to be non-crystalline. Measured density is in the range 1.904 and 2.304 g/cm³ and increased with Li_2O content. FTIR spectra revealed functional groups. Thermal properties were determined from DTA traces. DC conductivity is found increasing with temperature and Li_2O content. Mott's polaron hopping models were used to understand conductivity changes with temperature. Activation energy for conduction varied positively with Li_2O. The number of electronic states per unit volume around the Fermi energy was found to vary from 10^{31} to 10^{34} $ev^{-1}m^{-3}$. Dielectric parameters were measured over a wide range of temperature and frequency. Dielectric parameters decreased with frequency and increased with temperature. Analysis of the electric modulus indicated the nature of the conducting phase. In this paper, borosilicate systems mixed with CoO and Li_2O were thoroughly investigated for physical, thermal, conduction mechanisms and dialectical properties.

Keywords: Borosilicate glasses, glass transition temperature, conductivity, dielectric constant, impedance.

1. Introduction

The exceptional qualities of lithium borate glass, which are inseparable from its intricate and variable microstructure units, make it a popular choice for solid electrolytes, bioactive glass and other applications [1, 2]. Due to their useful mechanical properties, borosilicate glasses are used in cookware, laboratory glassware, and electronic and optical parts. The

* Department of Physics, Gulbarga University, Kalaburagi, Karnataka, India; talarisankarappa@gmail.com, aravinddyama@rediffmail.com, mandlepallavi17@gmail.com, mheera6@rediffmail.com

† K.L.E. Society's Basavaprabhu Kore Arts, Science and Commerce College, Chikodi. Belagavi district, Karnataka, India; ramannart@rediffmail.com

mechanical properties of these glasses are dependent on their chemical composition, namely the proportions of boron oxide (BO_3), silica (SiO_2) and modifiers such as alkali oxides. The structural integrity of borosilicate glasses is largely dependent on their network structure made of BO_3 and BO_4 units [3]. It is known that lithium reduces the melting temperature and improves the glass-forming capability and transparency of the glasses [4]. When a one cation (B or Li) is swapped for the other, keeping the overall modifier content constant, the systems exhibit mixed-glass former effect. The glass transition temperature and thermal stability rise in tandem with ionic conductivity. This helps in developing materials for applications in which high-performance electrolytes are required. Understanding the conduction mechanisms enables one to design optimised compositions to further enhance the desired properties [4, 5]. In solar selective absorbers, supercapacitors and lithium-ion batteries, the mixed valence states of cobalt ions (Co^{2+}/Co^{3+}) produce octahedral (oh) and tetrahedral (Td) geometric forms. Depending on the geometrical shape coordination of the Co^{2+} ions, the glass acquires a blue or pink hue [6].

Dielectric investigations on WO_3 and V_2O_5 doped borosilicate glasses have been reported [7]. The dielectric constant showed weak temperature dependence in the lower temperature region than at higher temperatures. Dielectric loss increased with temperature at all frequencies. Physical properties of lithium-borosilicate glasses have been extensively reported [8]. Mixed glass former effect has been observed in terms of ionic conductivity. Micro-structural and dielectric properties are reported for lead bismuth titanate brosilicate glass ceramics [9]. Both the dielectric parameters remained constant up to 200 °C and increased thereafter. Observed variations in dielectric parameters were attributed to the addition of La_2O_3, which promotes crystallization in the glass on heat treatment. Density, packing density, glass stability and ultrasonic velocity were found to increase with the increase in TiO_2 concentration. Based on the sizes of those properties, the glasses were proposed for dental and orthopaedic applications [10]. In our previous paper, conduction mechanisms operated in the present glasses have been analysed [11]. Lead-based borosilicate glasses were reported for electrical properties [12]. Mobility of Pb^{2+} ions in both borate and silicate networks has been extensively discussed in terms of dc conduction and its activation energy. The iron-doped sodium borosilicate glasses were probed for conductivity [13]. In these glasses, interestingly, the iron was recognised to be playing a modifier role, and the conduction mechanism was ionic rather than electronic.

The above-mentioned literature indicates that there are hardly any studies on borosilicate glasses containing both alkali and transition metal oxides. That is why the present paper is focused on a thorough investigation and analysis of functional groups in the network, thermal, dc conduction

and dielectric studies of novel borosilicate glasses having appreciable Li_2O content.

2. Experimental

Samples in the composition (80-x) B_2O_3 – $19SiO_2$ – 1CoO – xLi_2O were (x = 10, 15, 20, 25, 30, 35) produced by the melt quenching [14]. Analytical Reagent grade (Himedia make) B_2O_3, SiO_2, CoO and Li_2O were thoroughly mixed in defined ratios and were taken in crucibles made of silica and melted in a furnace up to 1300 K. The clean and highly homogenized melt developed was suddenly poured between two SS plates kept at room temperature. Samples have been annealed at 473 K in another furnace. The samples were collected and named as BSCL1, BSCL2, BSCL3, BSCL4, BSCL5 and BSCL6 glasses, respectively. XRD patterns of the powdered samples were recorded in a Proto X-ray diffractometer [15]. The transmittance was collected from an FTIR spectrometer in a Jasco spectrometer (IR-4600 (A)) for the wavenumber range 4000-400 cm^{-1} [11]. Density has been measured by the fluid displacement method of Archimedes. Using Xylene (= 0.865 g/cm^3) as an immersion liquid. DTA traces of the samples were obtained from a Hitachi-made instrument (STA 7300) in which high-quality argon has been used as the carrier gas. The powdered glasses weighing in the range 10-20 mg were placed in a pan made of alumina and heated from room temperature to 800 ^{0}C at the rate of 15K/min. During heating the DTA traces were recorded on a computer [15]. The well-shaped glasses of 3.5 mm thickness and cross-sectional areas in the range 46 mm2 - 61.5 mm2 were selected, and Silver paint was applied on their two parallel major surfaces. The two-point technique was followed, and resistance, R, for the temperature range 300K-523K was measured. A Chromel-Alumel K-type thermocouple was used to measure temperature within the error limit of ±1K. A voltage, V of 10V, was applied, and the current, I, flowing through the sample was noted at all the temperatures. Resistance R was calculated as (V/I). Resistivity, $\rho = \left(\frac{RA}{t}\right)$ and conductivity, $\sigma = 1/\rho$ were determined with A being the cross-sectional area of the glass and t the thickness of the glass [16]. The same set of samples were subjected to dielectric studies by measuring capacitance (C) and dissipation factor (tanδ) in an Impedance Analyser (WayneKerr 6500B), for the frequency range 50Hz - 1MHz and temperature range 300K – 573K [17].

3. Results and Discussion

3.1 XRD

The XRD patterns are shown in Figure 1. The non-crystalline nature is evident from the diffraction patterns as sharp peaks are absent. The two small, low-intensity peaks appearing around 42.15° and 43.41° have been indexed to be

(1,1,1) and (2,0,0) of CoO and B_2O_3 [3]. The grain sizes estimated from these two peaks are 26.04 nm and 15.27 nm, respectively. Due to the presence of nano-crystallites in the midst of a largely amorphous network, the present samples may be regarded as glass nanocomposites or ceramics.

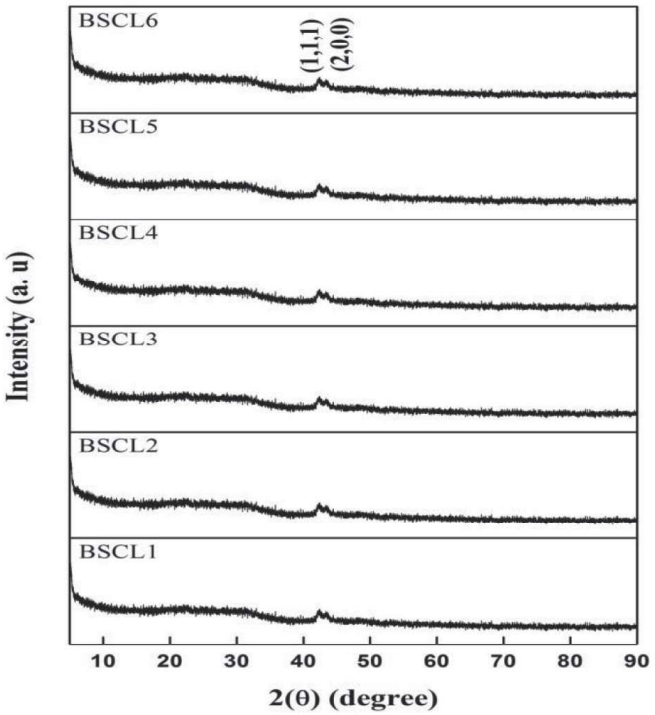

Figure 1: Powder XRD spectra.

3.2. FTIR

Functional groups in the glasses have been obtained from FTIR spectra (Figure 2). Eleven bands are observed for each glass. The observed bands are in the wave number ranges 418-444 cm^{-1}, 521-550 cm^{-1}, 647-679 cm^{-1}, 907-938 cm^{-1}, 1030-1076 cm^{-1}, 1340-1373 cm^{-1}, 1628-1651 cm^{-1}, 2253-2287 cm^{-1}, 2348-2385 cm^{-1}, 3421-3448 cm^{-1} and 3729-3783 cm^{-1}. A band detected at 418-444 cm^{-1} is allocated to bending vibrations of O–B–O [18, 19] and specific vibration of Li^+ [19]. Stretching vibrations of Co-O bonds are reflected in the band observed in the range 549–558 cm^{-1} [20]. The B-O-B bending vibrations are the cause for bands in the range 647–661 cm^{-1} [19]. The observed band at 907-938 cm^{-1} is identified to be due to undissociated carbonate (Li_2CO_3) species and B–O bond stretching in BO_4 units [18, 19]. The band seen at 1030-1076 cm^{-1} is due to stretching of BO_4 units due to the presence of Li^+ ions [18] and stretching vibrations of B-O bonds in BO_4 units from tri, tetra, penta-borate groups [21]. The bands located at 1340-1373 cm^{-1} is due to BO stretching vibrations of BO_3 units in meta borate groups [21]. The bands in the wavenumber range 1628-1651 cm^{-1} are recognized to originate from

the BO_3 unit converted from the tetrahedral BO_4 [21]. The bands present at 2253-2287 cm^{-1} are associated with O-H stretching vibration [21]. The bands observed at 2348-2385 cm^{-1} are assigned to the antisymmetric stretching of the water molecule [21]. The bands in the wavenumber range 3421-3448 cm^{-1} and 3729-3783 cm^{-1} are originating from O–H stretching in Hydroxyl groups and water molecules [18,21]. The observed bands and assignments given to them have been tabulated (Table 1).

Table 1: FTIR bands and their assignments

Band No. ↓	**Wavenumber (cm^{-1})**						**Band Assignments.**
Glass →	BSCL1	BSCL2	BSCL3	BSCL4	BSCL5	BSCL6	
1	444	435	423	438	419	418	Bending vibrations of O–B–O [18, 19] and Specific vibration of Li^+ [19].
2	546	548	549	549	521	550	Stretching vibrations of Co-O bonds [20].
3	647	672	679	678	678	678	B-O-B bonds bending vibration [19].
4	924	925	938	907	921	-	Undissociated lithium carbonate (Li_2CO_3) species and B–O stretching in BO_4 [18, 19].
5	1032	1030	1069	1076	1071	1068	Stretching of BO_4 units [18] and B-O in BO_4 from tri, tetra and penta borate groups [21].
6	1373	1364	1367	1340	1340	1365	Indications of B-O stretching in BO_3 units in meta borate groups [21].
7	1637	1651	1631	1628	1635	1637	Formation of BO_4 units from BO_3 [21].
8	2281	2287	2253	2253	2253	2253	O-H stretching vibration [21].
9	2363	2348	2364	2385	2385	2385	Antisymmetric stretching of water molecule [21].
10	3448	3447	3448	3422	3421	3421	Fundamental stretching of OH groups [21].
11	3756	3730	3729	3783	3758	3758	O–H stretching in hydroxyl groups [18].

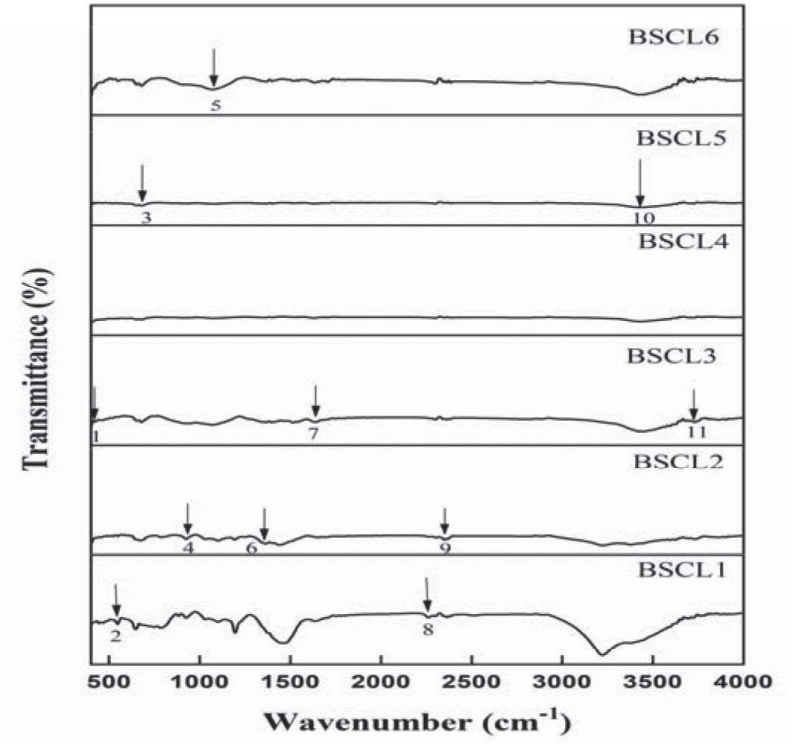

Figure 2: FTIR spectra of BSCL glasses. Down arrows indicate the identified bands.

3.3. Density and molar volume

The density (D) was estimated using $D=\left[\frac{W}{W-W_L}\right]\rho_L$. The weight in air, W and in Xylene, W_L, were measured experimentally. The density of Xylene, ρ_L was taken to be 0.88 g/cm^3. Density is found to be increased with Li_2O mole fractions and lies in the range 1.904 - 2.304 g/cm^3. The larger cation (Li) (size 0.076 nm) replacing the smaller one (B) may be the cause for the noticeable increases in D values. Molecular weight, M_w, of the glass and its molar volume, V_m, are related as $V_m = (M_w/D)$. The values of M_w for each glass were estimated using the set composition as per the procedure mentioned in [22]. The obtained V_m are in the range 56.95 cm^3/mol - 41.72 cm^3/mol. The obtained D and V_m are tabulated in Table 2. Figure 3 displays the Li_2O concentration dependence of D and V_m. It is evident that D increases and V_m decreases with Li_2O, which agrees with the results quoted in references [2, 23]. The ion concentration (N) was calculated using the formula, N = (xDNA)/MW, where Mw is the molecular weight and NA is Avogadro's number. The separation between the transition metal ions, $R = (1/N)^{1/3}$ was determined. The obtained values for N, R and r_p are recorded in Table 1. It can be seen that R decreases and N increases with x. The polaron radius (r_p) has been calculated using the equation $r_p = \frac{1}{2}\left(\frac{\pi}{6N}\right)^{\frac{1}{3}}$ [24]. The molar

volume is decreasing with Li_2O concentration, which indicates that the glass structure becomes closely packed [7]. The present D and V_m values are nearer to the reported ones for alkali-containing borate glasses [15, 23]. The polaron is made up of the electron and the surrounding lattice deformation, which causes the oxygen packing density and ionic concentration to drop. The lattice may therefore be thought of as a continuum as the deformation spans several lattice locations. It is anticipated that the conversion of BO_3 triangle units to BO_4 tetrahedral units will strengthen the glass's network connectivity, as evidenced by the density's monotonic increase [7, 18].

Table 2: Physical properties of BSCL glasses

SI. No.	Glasses	Density, D (g/cm^3)	Molar Volume (V_m) (cm^3/mol)	N x 10^{21} (cm^{-1}) ± 0.01	R (nm) ± 0.001	r_p (nm) ± 0.001
1.	BSCL1	1.904	56.95	1.057	98.15	0.395
2.	BSCL2	2.015	52.64	2.288	75.86	0.305
3.	BSCL3	2.126	46.74	3.945	63.28	0.255
4.	BSCL4	2.163	46.39	5.154	57.80	0.233
5.	BSCL5	2.262	45.8	6.454	53.72	0.216
6.	BSCL6	2.304	41.72	8.660	48.69	0.196

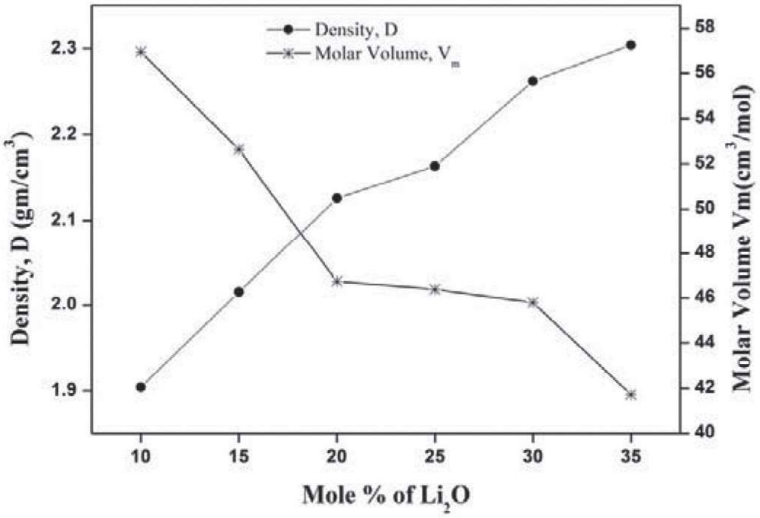

Figure 3: Composition dependence of D and V_m.

3.4. Thermal properties

The DTA traces of BSCL glasses are shown in Figure 4. Thermal characteristic parameters like transition temperature (T_g) and crystallization temperature (T_c) are determined as per endothermic dips as shown in the figure. Thermal stability, ΔT of the glasses has been estimated as ($\Delta T = T_c - T_g$).

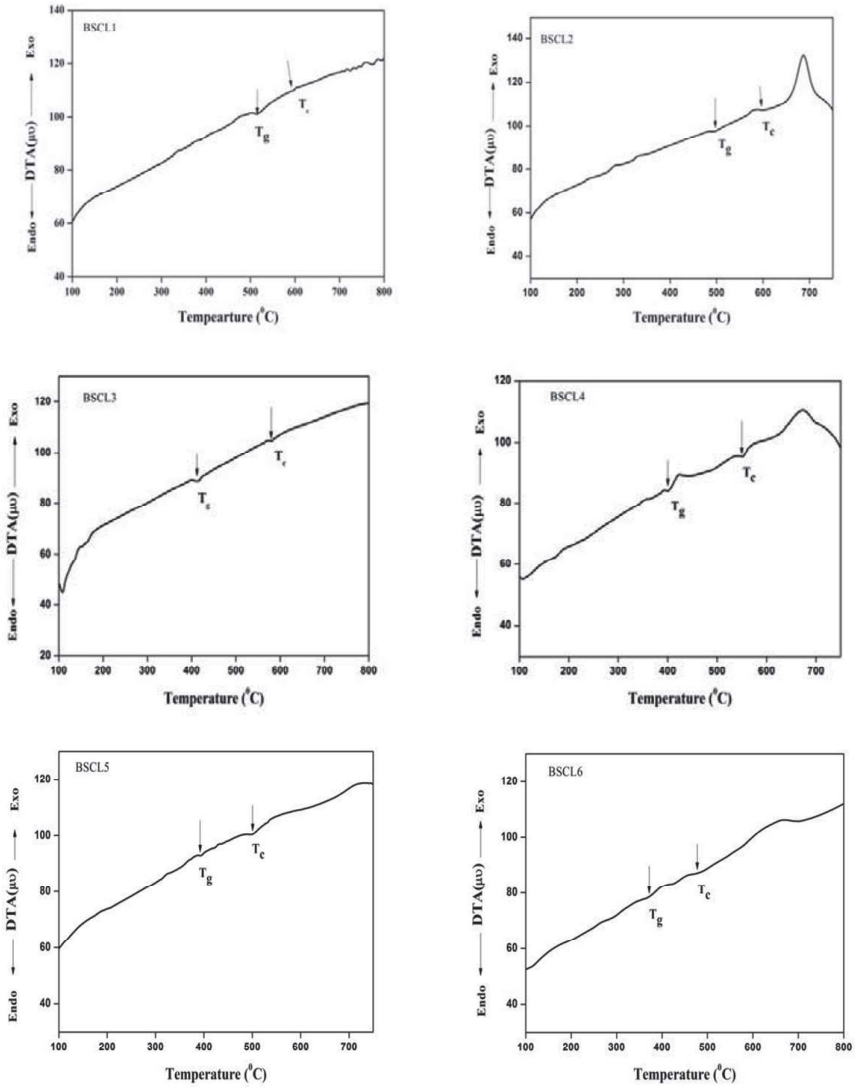

Figure 4: DTA traces of BSCL glasses

It is found that there is a decrease in T_g from 515 to 370 ^{0}C, and T_c from 596 to 473 ^{0}C and ΔT from 81 to 166 ^{0}C. It can be seen that the glass transition temperature T_g, decreases with an increase in Li_2O concentration. According to the earlier study, the glass transition temperatures decreased as the amount of network-forming oxides decreased [25]. When Li_2O is added to the glasses at the expense of network-forming oxide, it lowers the viscosity and cross-linking [9, 10]. This reduction in viscosity can significantly influence the processing and performance characteristics of the glass. Present results of T_g, T_c and ΔT (Table 3) highlight the crucial role played by Li2O in optimizing thermal properties [14, 25].

Table 3: Thermal parameters of BSCL glasses

SI. No.	Glass	T_g (°C) ± 1	T_c (°C) ± 1	ΔT (°C) ± 1
1.	BSCL1	515	596	81
2.	BSCL2	498	597	99
3.	BSCL3	413	579	166
4.	BSCL4	402	550	148
5.	BSCL5	393	501	131
6.	BSCL6	370	473	103

3.5 Electrical conductivity

Measured electrical resistance (R) was used to determine conductivity (σ). The obtained σ values are in the range $1.69x10^{-3}$ $\Omega^{-1}m^{-1}$ to $9.90x10^{-5}$ $\Omega^{-1}m^{-1}$. The conductivity increased as the temperature increased, indicating a semiconducting nature. This finding is in agreement with a number of other TMI and alkali mixed glasses [11]. The conductivity changes with temperature were understood using Mott's SPH model. At high temperatures, the conductivity data have been fit to the expression, $\sigma = (\sigma_o/T) \exp(-W/k_B)$. The terms in it have the same meaning as stated in [12, 26]. SPH plots of ln(σT) versus reciprocal temperature are shown in Figure 5. Lines indicate linear fits at high temperature. The gradients of the linear fits gave activation energy (W). Obtained W values are recorded in Table 4. The low-temperature data falling outside the SPH fit will have variable activation energy with temperature [16]. The obtained W are found to be in the range 0.058 eV - 0.514 eV and increase with Li_2O content.

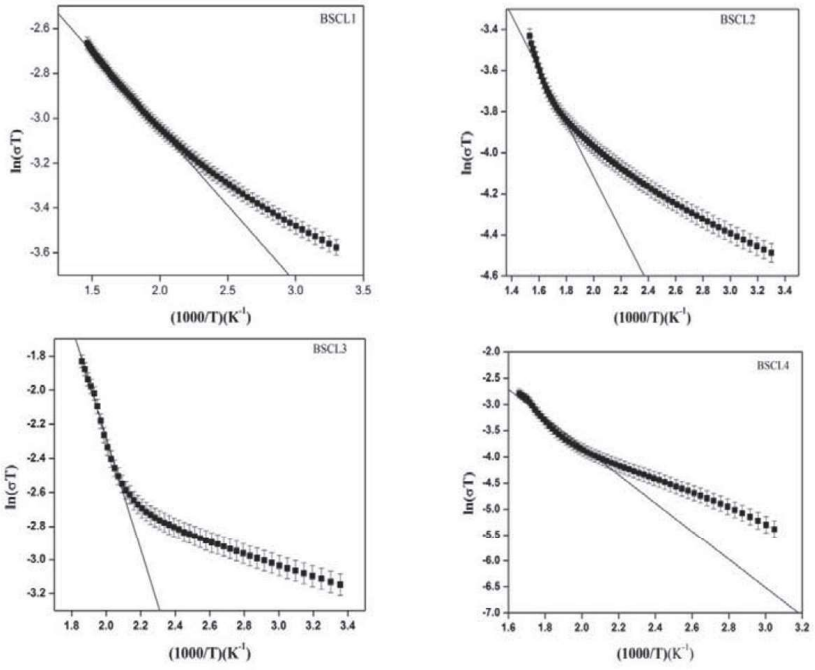

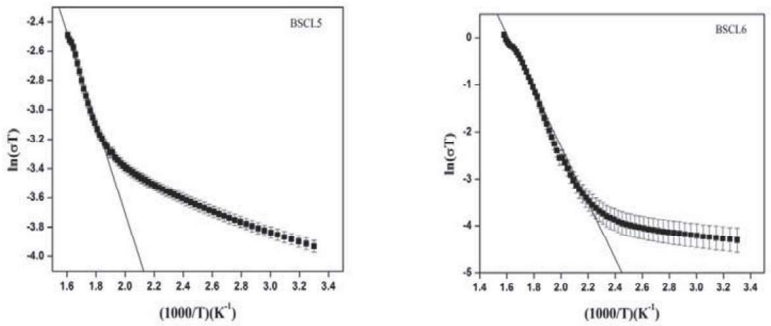

Figure 5: SPH plots of ln(σT) versus reciprocal temperature. Lines are linear fits at high temperature.

The Variable Range Hopping model of Mott (MVRH) has been applied to the data at T‹ T_D. T_D is the temperature at which the conductivity deviates from Mott's SPH Model prediction. The conductivity as per MVRH is given as [27, 28], $\sigma = A \exp(-B/T^{-1/4})$. Where the constants A and B are defined in [27, 28].

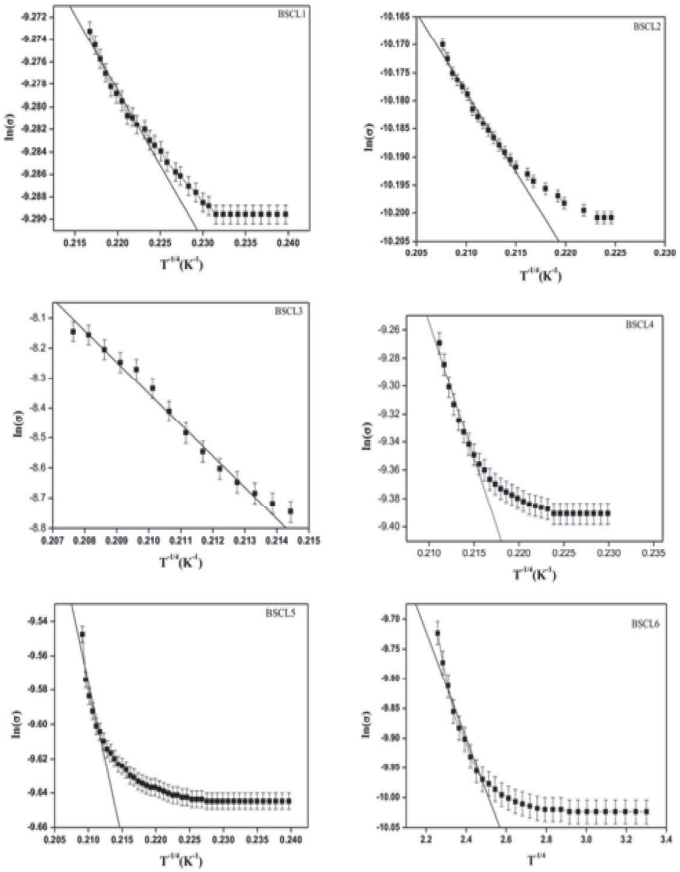

Figure 6: ln(σ) versus ($T^{-1/4}$) as per MVRH model and linear fits are shown as solid lines.

The MVRH plots of ln(σ) versus ($T^{-1/4}$) are shown in Figure 6. The linear fits shown in the figure gave A and B. Using B, the number of electron states per unit volume at the Fermi level, $N(E_F)$ were estimated by taking $\alpha = 2x10^{10}$ [11], and the obtained results are tabulated in Table 4. The $N(E_F)$ values obtained from the MVRH model fit are in the range 10^{26} to 10^{29} ev^{-1} cm^{-3}. These are comparable with reported ones for B_2O_3-Na_2O-CaO-AgCl-Li_2O [26], B_2O_2-TeO_2-CoO-Li_2O glasses [15] and Li_2O-SiO_2-B_2O_3-ZnO-WO_3 [11]. So, the MVRH model can be taken to be enough to understand conductivity at low temperatures.

Table 4: Values of W and $N(E_F)$ obtained from SPH and VRH model fits.

Glass	σ ($\Omega^{-1}m^{-1}$) at (538K)	W (eV)	$N(E_F)$ $eV^{-1}cm^{-3}$
BSCL1	$9.999x10^{-5}$	0.0589	5.28×10^{29}
BSCL2	$3.830x10^{-5}$	0.1128	2.60×10^{29}
BSCL3	$2.978x10^{-4}$	0.2658	1.40×10^{27}
BSCL4	$1.118x10^{-4}$	0.2829	1.21×10^{27}
BSCL5	$7.361x10^{-5}$	0.3122	1.52×10^{27}
BSCL6	$3.998x10^{-4}$	0.5146	1.76×10^{26}

3.6. Dielectric properties

The parameters ε′, and ε′′have estimated by substituting C and tanδ in the relations $\varepsilon' = \left(\frac{Cd}{\varepsilon_0 A}\right)$ and ε'' = ε' tanδ [28]. The obtained ε′ and ε′′ are in the range 10 - 10^3 and 10 -10^5, respectively, and they are comparable with results in reference [13]. Temperature and frequency-dependent variations of ε′ and ε′′ are sketched for BSCL2 glass in Figure 7. Both the parameters vary positively with temperature and frequency. The remaining glasses under the present study exhibited similar trends. Rise in temperature suppresses molecular interactions and facilitates orientational vibrations, and that in turn increases ε′ [17]. Also, a larger number of NBOs are produced when lithium ions are incorporated, leading to the polarization of space charges and that increases ε′. At low frequencies ε′ is high because of all three polarizations; ionic, electronic and orientational present. Contributions from the ionic and orientation side vanish at higher frequencies.

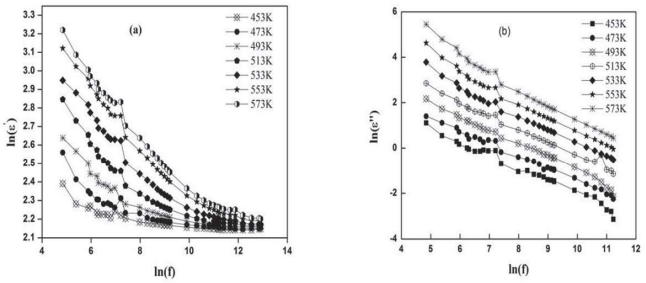

Figure 7: Frequency (f) and temperature dependencies of (a) ε′ and (b) ε′′ for BSCL2-glass.

3.7. Modulus (M) Analysis

M′ and M′′ of M (= M' + i M'') have been estimated as the relations mentioned in [26]. Figure 8 (a) & (b) display changes in M' and M'' with frequency and temperature BSCL2 glass. Like in other glasses [30, 31], the M' is constant up to a certain frequency and increases thereafter, for all T. M' reaches M_{max} at some frequency. A small value of M' at lower frequencies implies that electrode polarization contributes minimally at these frequencies, and conductivity relaxation plays the role [32]. With an increase of T, the M_{max} reduces because of the presence of lithium. M' behaviour with frequency is observed to be same for the remaining glasses as that of BSCL2 glass.

In Figure 8(b), it **can be noticed that** M''_{max} shifts to a higher frequency with the increase of temperature. Peaks in M'' spectra reveals that the conductivity relaxation process is in operation. The peak is an indication that the polaron's mobility has been confined to a short range. Below peak frequency, polarons are only able to move within a potential range. Other samples of the series exhibited similar frequency dispersion of M''. These observations agree with reports on Li_2O-B_2O_3- SiO_2-Li_2SO_4 [33].

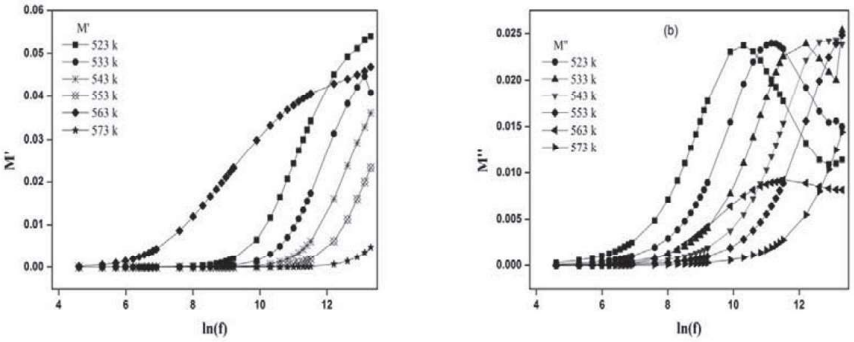

Figure 8: Frequency dispersion of (a) M' for BSCL2 glass and (b) M'' for BSCL1 glass.

3.8. Impedance, Z (= Z'+iZ") Analysis

Figure 9 shows Z" versus Z' at different T for BSCL2. The graph shows semicircles with varying diameters at varying temperatures. Our other glasses had the same trends, suggesting a single-phase nature [34]. The Z'_{max} appears at a higher frequency for higher temperatures. This demonstrates that the electrical relaxation phenomena are brought in by an increase in conductivity or a fall in resistance with temperature. Semicircles are shrinking with temperature, hinting at a temperature-dependent relaxing process occurring in the samples [35, 36].

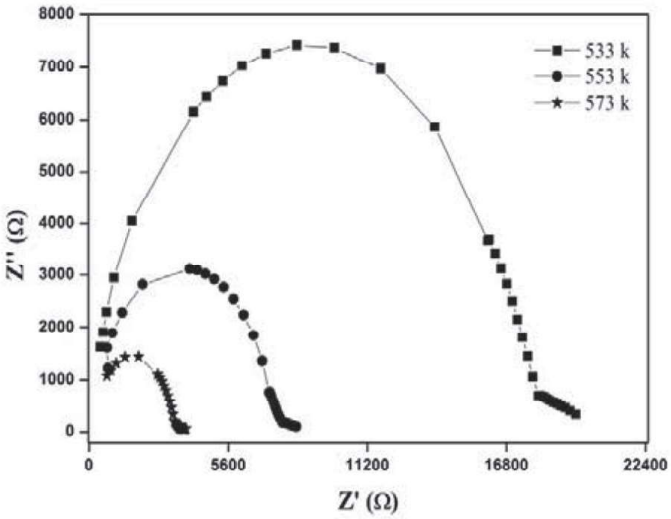

Figure 9: Z" versus Z' for BSCL2 glass at different temperature

4. Conclusions

i) Due to the presence of small peaks in XRD spectra, the samples are confirmed to be glass ceramics or nano composites.

ii) Density increased, and Molar volume decreased with Li_2O. It indicates that the tight packing of the glass network is happening with the increase of Li_2O content.

iii) The functional groups present in the glasses were obtained from FTIR. The T_g and T_c increased with Li_2O concentration. Appreciable thermal stabilities have been exhibited by these samples.

iv) Increasing trend of conductivity with temperature indicated semiconducting behaviour.

v) High temperature conductivity varied as per Mott's SPH model, and that of low temperature conductivity as per MVRH models. Activation energy for conductivity and the number of electronic states at the Fermi energy were determined.

vi) Frequency dispersions observed in ε′, and ε″ were explained in terms of different polarization effects. The impedance and electric moduli spectra of the glasses have been thoroughly analysed.

vii) The Z" versus Z' plots confirmed the existence of single conducting phase in the present samples.

In total, the presently studied glasses having appreciable Li_2O content measured sizable ionic conductivity and medium range dielectric properties are suitable for energy storage applications after further exploring them for chemical durability and extensive thermal stability studies.

Acknowledgement:

The corresponding author, Prof. T. Sankarappa acknowledges the rigorous research training received from Prof. Michael Springford and Prof. Philip Meeson at H H Wills Physics laboratory, Bristol University, United Kingdom.

Author Contributions:

Aravind Dyama conducted experiment, analyzed data, carried out analyses and drafted the article

T. Sankarappa postulated the concept, supervised the work, provided the facilities and edited the article

Pallavi Jamadar, Mohansingh. H, R. Ramanna helped in the experiment, analysis of the data and drafting the article

Conflict of interest statement:

There is no conflict of interest among the authors concerning the present work

Funding Statement

There was no funding from any agency for the research work presented in this paper.

References

[1]. Ganvir, V. Y., and R. S. Gedam. "Effect of La2O3 addition on structural and electrical properties of sodium borosilicate glasses." *Materials Research Express* 4, no. 3 (2017): 035204.

[2]. Song, Lulu, Yunxia Wang, Alex C. Hannon, Steve Feller, Wu Li, Yongquan Zhou, and Fayan Zhu. "Structural investigation of lithium borate glasses by Raman spectroscopy: Quantitative evaluation of structural units and its correlation with density." *Journal of Non-Crystalline Solids* 616 (2023): 122478.

[3]. Marzouk, M. A., R. M. Bahaa, M. E. Hassaneen, and A. M. Othman. "Investigating CoO Doping in Sodium Magnesium Borosilicate Glasses: Impacts on Structural, Thermal, Optical, and Mechanical Properties." *Journal of Electronic Materials* 54, no. 4 (2025): 3280-3294.

[4]. Vijayalakshmi, L., K. Naveen Kumar, G. Bhaskar Kumar, and Pyung Hwang. "Structural, dielectric and photoluminescence properties of Nd3+ doped Li2O-LiF-B2O3-ZnO multifunctional optical glasses for solid state laser applications." *Journal of Non-Crystalline Solids* 475 (2017): 28-37.

[5]. Abdel-Galil, A., N. L. Moussa, and O. I. Sallam. "Dual role of CoO and electron beam irradiation in enhancement the transport properties of borate glasses." *Ceramics International* 50, no. 2 (2024): 3187-3198.

[6]. Taha, Eman O., and Aly Saeed. "The effect of cobalt/copper ions on the structural, thermal, optical, and emission properties of erbium zinc lead borate glasses." *Scientific Reports* 13, no. 1 (2023): 12260.

[7]. Thombre, D. B., and Megha D. Thombre. "Study of physical properties of lithium borosilicate glasses." *International Journal of Engineering Research and Development* 10, no. 7 (2014): 9-19.

[8]. Nagaraja, N., T. Sankarappa, and M. Prashant Kumar. "Electrical conductivity studies in single and mixed alkali doped cobalt–borate glasses." *Journal of Non-Crystalline Solids* 354, no. 14 (2008): 1503-1508.

[9]. Gautam, Chandkiram R., Abhishek Madheshiya, and Ranabrata Mazumder. "Preparation, crystallization, microstructure and dielectric properties of lead bismuth titanate borosilicate glass ceramics." *Journal of Advanced Ceramics* 3, no. 3 (2014): 194-206.

[10]. Shaaban, Kh S., B. M. Alotaibi, Nuha Alharbiy, Ateyyah M. Al-Baradi, and AF Abd El-Rehim. "Impact of TiO2 on DTA and elastic moduli of calcium potassium borophosphosilicate glasses in prelude for use in dental and orthopedic applications." *Silicon* 14, no. 17 (2022): 11991-12000.

[11]. Dyama, A., T. Sankarappa, M. Heerasingh, A. Devidas, P. Jamadar, and A. Malge. "Study of Conduction Mechanisms in Alkali and Transition Metal Oxides Doped Borosilicate Glasses." *Indian Journal of Science and Technology* 17, no. 17 (2024): 1767-1775.

[12]. El-Damrawi, G., and E. Mansour. "Electrical properties of lead borosilicate glasses." *Physica B: Condensed Matter* 364, no. 1-4 (2005): 190-198.

[13]. Ciżman, A., E. Rysiakiewicz-Pasek, M. Krupiński, M. Konon, T. Antropova, and M. Marszałek. "The effect of Fe on the structure and electrical conductivity of sodium

[14]. Heerasingh, Mohansingh, T. Sankarappa, Amarkumar Malge, Ashwini Devidas, Pallavi Jamadar, B. Raghavendra, and Aravind Dyama. "Electrical Conduction Mechanisms and Radiation Shielding Parameters of H2WO4-Doped Lead Vanadate Glasses." *Journal of Electronic Materials* (2025): 1-11.

[15]. Ashwajeet, J. S., T. Sankarappa, T. Sujatha, and R. Ramanna. "Thermal and electrical properties of (B2O3-TeO2-Li2O-CoO) glasses." *Journal of Non-Crystalline Solids* 486 (2018): 52-57.

[16]. Malge, Amarkumar, T. Sankarappa, T. Sujatha, P. Abdul Azeem, G. B. Devidas, and Santoshkumar Kori. "Structural and DC conductivity studies of borotellurite glasses doped with ZnO, Li2O and Dy2O3." *Materials Today: Proceedings* 26 (2020): 1960-1963.

[17]. Heerasingh Mohansingh, T. Sankarappa, Amarkumar Malge, Ashwini Devidas, B. Raghavendra, Jamadar Pallavi, and Aravind Dyama. "Dielectric, thermal and gamma shielding characteristics of PbO–TeO2–V2O5–CoO glasses." *Materials Chemistry and Physics* 307 (2023): 128200.

[18]. Malge, Amarkumar, T. Sankarappa, T. Sujatha, and G. B. Devidas. "Structural, Dielectric and AC Conductivity of Multicomponent Borotellurite Glasses." *Glass Physics and Chemistry* 47, no. Suppl 1 (2021): S1-S9.

[19]. Kaky, Kawa M., G. Lakshminarayana, S. O. Baki, Y. H. Taufiq-Yap, I. V. Kityk, and M. A. Mahdi. "Structural, thermal, and optical analysis of zinc boro-aluminosilicate glasses containing different alkali and alkaline modifier ions." *Journal of Non-Crystalline Solids* 456 (2017): 55-63.

[20]. Rajyasree, Ch, S. Bala Murali Krishna, A. Ramesh Babu, and D. Krishna Rao. "Structural impact of cobalt ions on BaBiBO4 glass system by means of spectroscopic and dielectric studies." *Journal of Molecular Structure* 1033 (2013): 200-207.

[21]. Selvi, S., K. Marimuthu, and G. Muralidharan. "Effect of PbO on the B2O3–TeO2–P2O5–BaO–CdO–Sm2O3 glasses-structural and optical investigations." *Journal of Non-Crystalline Solids* 461 (2017): 35-46.

[22]. Kumar, B. Vijaya, T. Sankarappa, M. Prashant Kumar, and Santosh Kumar. "Electronic transport properties of mixed transition metal ions doped borophosphate glasses." *Journal of non-crystalline solids* 355, no. 4-5 (2009): 229-234.

[23]. El-Alaily, N. A., and R. M. Mohamed. "Effect of irradiation on some optical properties and density of lithium borate glass." *Materials Science and Engineering: B* 98, no. 3 (2003): 193-203.

[24]. Paz, E. C., J. D. M. Dias, G. H. A. Melo, T. A. Lodi, J. O. Carvalho, P. F. Façanha Filho, M. J. Barboza, F. Pedrochi, and A. Steimacher. "Physical, thermal and structural properties of Calcium Borotellurite glass system." *Materials Chemistry and Physics* 178 (2016): 133-138.

[25]. Taha, T. A., and A. S. Abouhaswa. "Structure, optical and magnetic properties of barium sodium borate/cobalt oxide glass structures." *Optical and Quantum Electronics* 55, no. 6 (2023): 483.

[26]. Mastanappa, Ashok, Shrikant Biradar, G. B. Devidas, R. Rajaramakrishna, M. I. Sayyed, and M. N. Chandrashekara. "Effect of Li2O on physical, structural, thermal, optical, and electrical properties of mixed alkali borate glasses containing silver nanoparticles." *Optical Materials* 157 (2024): 116224.

[27]. Heerasingh, Mohansingh, T. Sankarappa, Amarkumar Malge, Ashwini Devidas, B. Raghavendra, Jamadar Pallavi, and Aravind Dyama. "Physical and electrical studies of tellurite-lead-vanadate glasses doped with CoO." *Materials Today: Proceedings* 100 (2024): 25-30.

[28]. Murugasen, Priya, Deepa Shajan, and Suresh Sagadevan. "A study of structural, optical and dielectric properties of Eu2O3 doped borate glass." *International journal of physical Sciences* 10, no. 20 (2015): 554-561

[29]. Gedam, R. S., and D. D. Ramteke. "Electrical, dielectric and optical properties of La2O3 doped lithium borate glasses." *Journal of Physics and Chemistry of solids* 74, no. 7 (2013): 1039-1044.

[30]. Sheoran, A., S. Sanghi, S. Rani, A. Agarwal, and V. P. Seth. "Impedance spectroscopy and dielectric relaxation in alkali tungsten borate glasses." *Journal of Alloys and compounds* 475, no. 1-2 (2009): 804-809.

[31]. Dyama, Aravind, T. Sankarappa, Mohansingh Heerasingh, Jamadar Pallavi, Rohini Kalmath, Dawalappa B. Husenkhan, and Jyoti Kattimani. "Structural,

thermal, optical and dielectric properties of borosilicate glass composites containing tungsten, zinc and lithium oxides." *Physica Scripta* 100 (2025) 105925.

[32]. Mundher, M., A. A. Bendary, M. A. Farag, Abu Bakr El-Bediwi, and M. Y. Hassaan. "Tungsten oxide effects on conductivity, dielectric parameters, and density of sodium germanium borosilicate glass." *Journal of Materials Science: Materials in Electronics* 34, no. 12 (2023): 1069.

[33]. Gundale, S. S., V. V. Behare, and A. V. Deshpande. "Study of electrical conductivity of Li2O-B2O3-SiO2-Li2SO4 glasses and glass-ceramics." *Solid State Ionics* 298 (2016): 57-62.

[34]. Kupracz, Piotr, Jakub Karczewski, Marta Prześniak-Welenc, N. A. Szreder, Michał Jerzy Winiarski, Tomasz Klimczuk, and R. J. Barczy'nski. "Microstructure and electrical properties of manganese borosilicate glasses." *Journal of Non-Crystalline Solids* 423 (2015): 68-75.

[35]. Jayswal, Manish S., D. K. Kanchan, Poonam Sharma, and Meenakshi Pant. "The effect of PbI2 on electrical conduction in Ag2O-V2O5-B2O3 superionic glass system." *Solid State Ionics* 186, no. 1 (2011): 7-13.

[36]. Barczyński, Ryszard Jan, Paulina Król, and Leon Murawski. "Ac and dc conductivities in V2O5–P2O5 glasses containing alkaline ions." *Journal of non-crystalline solids* 356, no. 37-40 (2010): 1965-1967.